Pergamon

Bioorganic & Medicinal Chemistry 8 (2000) 201–214

BIOORGANIC & MEDICINAL CHEMISTRY

Ligand Design for α_1 Adrenoceptor Subtype Selective Antagonists

John B. Bremner, [a,*] Burak Coban, [a,†] Renate Griffith, [a]
Karina M. Groenewoud [b] and Brian F. Yates [b]

[a]*Department of Chemistry, University of Wollongong, Northfields Ave, Wollongong, NSW 2522, Australia*
[b]*Department of Chemistry, University of Tasmania, Hobart, TAS 7005, Australia*

Received 19 March 1999; accepted 15 September 1999

Abstract—α_1 Adrenoceptors have three subtypes and drugs interacting selectively with these subtypes could be useful in the treatment of a variety of diseases. In order to gain an insight into the structural principles governing subtype selectivity, ligand based drug design (pharmacophore development) methods have been used to design a novel 1,2,3-thiadiazole ring D analogue of the aporphine system. Synthesis and testing of this compound as a ligand on cloned and expressed human α_1 adrenoceptors is described. Low binding affinity was found, possibly due to an unfavourable electrostatic potential distribution. Pharmacophore models for antagonists at the three adrenoceptor sites (α_{1A}, α_{1B}, α_{1D}) were generated from a number of different training sets and their value for the design of new selective antagonists discussed. The first preliminary antagonist pharmacophore model for the α_{1D} adrenoceptor subtype is also reported.

Introduction

The α_1 adrenoceptors (α_1 ARs) mediate many effects of the sympathetic nervous system. Like other adrenergic receptors, α_1 ARs are activated by the catecholamines, adrenaline and noradrenaline.[1] The α_1 ARs are membrane proteins and members of the G-protein coupled receptor superfamily. Three distinct subtypes, α_{1A}, α_{1B} and α_{1D}, have been confirmed by cloning techniques.[2–5]

The α_1 ARs have divergent affinities for many synthetic drugs. Drugs interacting selectively as agonists, or as antagonists, with the subtypes have been used in the treatment of a variety of diseases including hypertension, asthma and prostatic hypertrophy.[6,7] Ligands showing very high binding selectivity for the α_{1A} subtype over both α_{1B} and α_{1D} (>3000-fold) are available.[8] However, these ligands (SNAP compounds, derived from niguldipine) usually do not distinguish very well between the α_{1B} and α_{1D} subtypes (see Table 1 and Fig. 1 for examples, compounds **9**–**12**). For the α_{1B} subtype, the best reported selectivity is achieved by (+)-cyclazosin (**2**) (100-fold over α_{1A}, Table 1). For the α_{1D} subtype the situation is not much better, with the highest selectivity of about 200-fold over α_{1A} binding, being reported for a compound from the group at Synaptic Pharmaceutical Corporation[9] (**25**, Table 1).

In order to design selective antagonists, a ligand-based drug design (pharmacophore development) method may be used by means of Catalyst software of Molecular Simulations, Inc. (MSI). This method is applicable when the three-dimensional structure of the receptor is unknown and a series of compounds has been identified that show the activity of interest. The aim of this approach is to identify a pharmacophore, which is a template derived from the structures of these compounds, and representing the geometry of the receptor site as a collection of functional groups in three-dimensional space.

A pharmacophore for antagonists at the α_1 AR has been reported.[21] Considering a wide variety of chemical structures, features linked with α_1 AR antagonism were noted. This study was based on a process which involved choosing an active, conformationally constrained molecule as a template to be compared with the conformationally flexible compounds. The resulting pharmacophore had three features including an aromatic region, a basic nitrogen and a semi-polar region or a bulky lipophilic area.[21] However, this early study did not consider specific requirements for α_1 AR subtypes.

Keywords: drug design; aporphine analogues; adrenergic receptors; selectivity.
*Corresponding author. Tel.: +61-2-4221-4256; fax: +61-2-4221-4287; e-mail: john_bremner@uow.edu.au
†Current address: Karaelmas Universitesi, Fen-edebiyat Fakultesi, Kimya Bolumu, Zonguldak, Turkey.

0968-0896/00/$ - see front matter
PII: S0968-0896(99)00263-1

Table 1. Anatagonists and their activities

No.	Compound name	Activity K_i(nM)			Selectivity			Ref
		α_{1A}	α_{1B}	α_{1D}	B/A	D/A	B/D	
1	Prazosin	0.2	0.25	0.32	1.25	1.6	0.78	10
2	Cyclazosin	12	0.13	3.2	0.01	0.27	0.04	11
3	Abanoquil	0.04	0.08	0.04	2	1	2	7
4	REC-15/2615	1.9	0.3	2.6	0.16	1.37	0.12	12
5	Alfuzosin	10	10	3.16	1	0.32	0.32	13
6	Doxazosin	3.16	1.0	4.0	0.32	1.29	0.25	13
7	Terazosin	6.3	2.0	2.5	0.32	0.40	0.80	13
8	Bunazosin	0.5	1.0	1.0	2	2	1	14
9	(+)-Niguldipine	0.15	55	100	367	667	0.55	13
10	SNAP-5089	0.23	13	66	56.5	287	0.24	13
11	SNAP-5399	0.65	324	631	498	971	0.51	13
12	SNAP-5150	1.9	331	400	174	211	0.83	13
13	WB-4101	0.16	2.5	0.25	15.6	1.56	10	10
14	Phentolamine	1.6	7.9	7.9	4.9	4.9	1	15
15	5-Methyluropidil	0.63	40	10	63.5	15.9	4	13
16	KMD-3213	0.04	20	2.0	500	50	10	13
17	AH-11110A	2500	76	2750	0.03	1.1	0.03	16
18	BMY-7378	250	630	6.3	2.52	0.03	100	13
19	SKF-104856	44	63	5.2	1.43	0.12	12.1	17
20	Discretamine	616	360	25	0.58	0.04	1.44	18
21	Corynanthine	142	517	253	3.64	1.78	2.04	4
22	Benzoxathian	0.2	4.0	0.4	20	2	10	19
23	Spiperone	7.9	0.5	13	0.06	1.65	0.04	19
24	(+)-YM-617	4.3	96	22	22.3	5.12	4.36	15
25	SNAP-8719	294	191	1.6	0.65	0.00	119	9
26	Indoramin	4.0	40	160	10	40	0.25	13
27	RS-17053	0.6	16	16	26.7	26.7	1	13
28	A-131701	0.22	6.95	0.97	31.6	4.41	7.16	10
29	NAN-190	2.0	15	0.8	7.50	0.40	18.8	17
30	WAY-100635	144	186	63	1.29	0.44	2.95	17
31	RS-100,975	1.0	79	100	79	100	7.9	13
32	REC-15/2739	1.0	32	2.5	32	2.5	12.8	13
33	SNAP-1069	16	200	790	12.5	49.4	0.25	13
34	SL-89.0591	2.5	13	2.5	5.20	1	5.20	13
35	JHT-601	0.4	1.2	1.2	3	3	1	13
36	GG-818	0.2	16	25	80	12.5	0.64	13
37	Uropidil	288	1320	1660	4.58	5.76	0.80	17
38	Bromotopsentin	12000	740	—	0.06			20

A number of linear QSAR models have also been developed from α_1 AR antagonists.[22–24] Complete geometry optimisation was performed for the protonated forms of the compounds considered, taking the extended conformations as starting geometries.[22] This study strongly suggested that the protonated amine function is very important for binding. In addition, two aromatic systems on either side of the nitrogen (at 4–7 Å) are also necessary for the activity, although no clear trend was observed for the angle between these three features. In the other studies a protonated amine function was also found to be a crucial element of the α_1 AR antagonists.[23,24]

In our earlier ligand-based pharmacophore study,[25] α_{1A} and α_{1B} AR pharmacophore models were developed by using Apex-3D software of MSI. These models were the first subtype specific α_1 AR pharmacophores reported, and they also indicated the importance of a protonated amine. The additional features of the models were an aromatic ring and a polar region for both subtypes. The only difference between the pharmacophores for the two subtypes was the distance between the aromatic ring and the amine function. This distance was shorter for the α_{1A} subtype. Based on this data, a 1,2,3-thiadiazole ring D-aporphine analogue (**39**) (see Scheme 1) was designed with expected selectivity for the α_{1A} AR over the α_{1B} subtype. The short distance between the basic nitrogen and the aromatic ring did not allow **39** to map effectively on the α_{1B} pharmacophore model. Synthesis and binding studies of **39** on cloned and expressed human α_1-adrenoceptors are discussed in the current paper.

Compound **39** is an analogue of the aporphine alkaloid system,[26] in which ring D is replaced by a 1,2,3-thiadiazole ring. Aporphine alkaloids such as boldine and glaucine have shown α_{1A} selective binding,[27] and an aporphine ring D indole analogue, IQC (**40**),[28] has shown high affinity for α_1 AR sites.

Since the publication of our original study,[25] several important subtype selective α_1 AR antagonists have been developed and the selectivity of risperidone has been queried. Even though risperidone was listed as an α_{1B} selective antagonist in an earlier paper,[29] this selectivity was questioned in another study,[11] which found it to be only slightly selective for the α_{1A} subtype over α_{1B}. In addition, it has been found experimentally that niguldipine analogues (which were in the training set of the previous study[25]) bind at a different binding site of the receptor.[29] This was supported by a later

study and it was suggested that they bind to the same aspartate residue but the other interacting residues are different to those for the other antagonists.[30] One of the aims of the current study was to investigate the structural features of this important class of α_{1A} selective agents and compare them to the features encountered in other α_{1A} selective agents, such as KMD-3213 (**16**, Table 1 and Fig. 1), with a view to contributing to the understanding of the interaction of these compounds with α_1 ARs. In the case of the quinazoline derivatives and close analogues **1**–**8**, such as prazosin, we have already stated our belief[25] that these compounds also may bind to a different site on the α_1 ARs. This class of compounds, with the notable exception of (+)-cyclazosin, is characterised by very high affinity for all three α_1 AR subtypes, with no selectivity between them. Furthermore, the Apex-3D program has been superseded by Catalyst. It was thus necessary to re-examine the pharmacophores and this was done using the updated software. Inclusion of further selective antagonists described since the Apex-3D work was also undertaken, together with an extension to α_{1D} antagonists.

Results

Synthesis of the thiadiazole aporphine analogue 39 and of IQC 40

The synthesis of racemic **39** was performed via the intermediate tricyclic ketone **47** (Scheme 1). The carbonyl

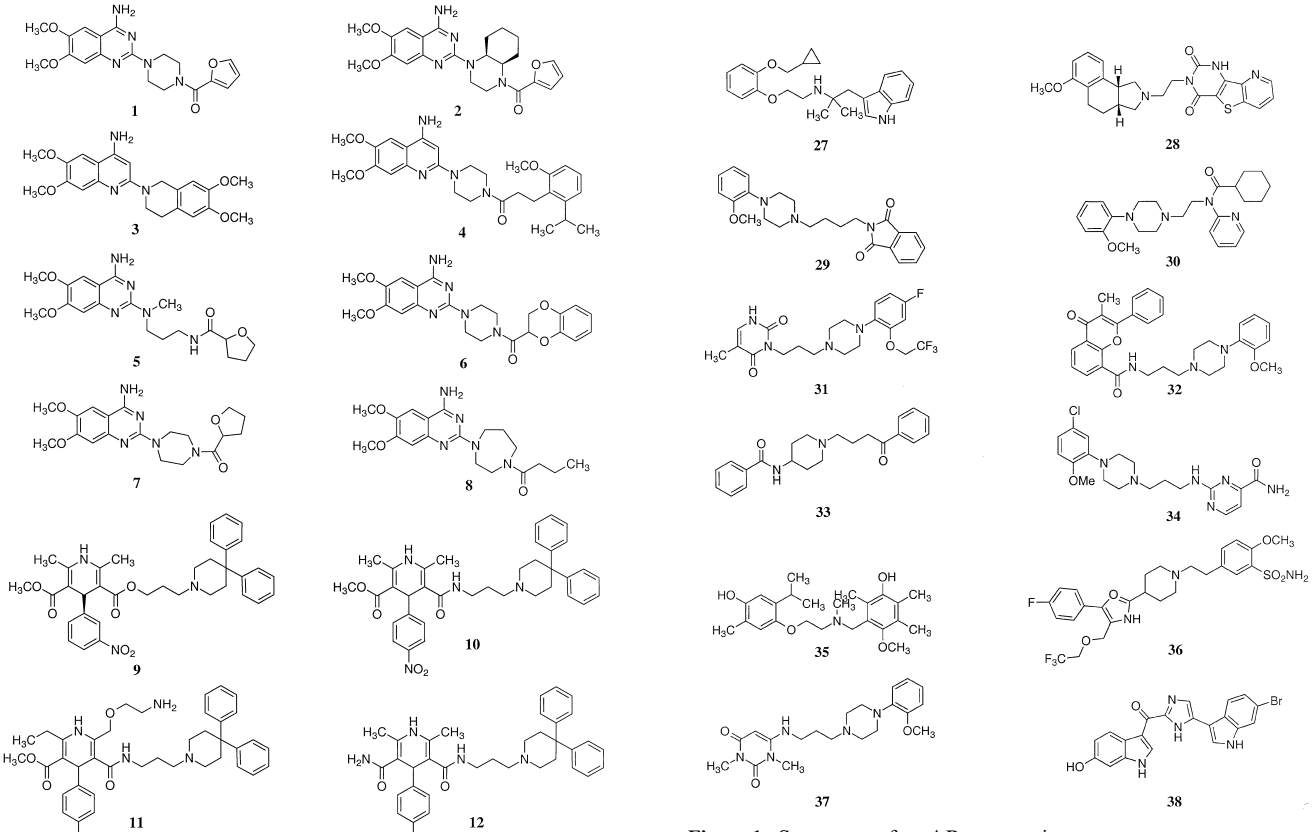

Figure 1. Structures of α_1-AR antagonists.

group in the 7-position was then used to build the D ring. The multi-step sequence for the synthesis of **47** involved an isoquinoline precursor **41**, which was prepared by the method of Brossi et al.[32] The *N*-propyl

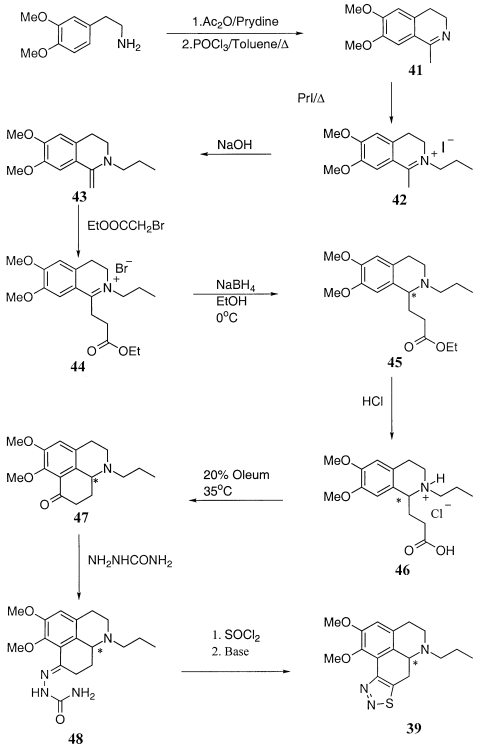

Scheme 1. Preparation of racemic **39**.

derivative **42** was prepared in a sealed tube at 90 °C in 90% yield. The bromide salt ester derivative **44** could then be made using the freshly prepared enamine derivative **43** after exposure of the iodide salt **42** to strong base. The reduction of **44** and the preparation of the amino acid hydrochloride salt derivative **46** was achieved in over 90%

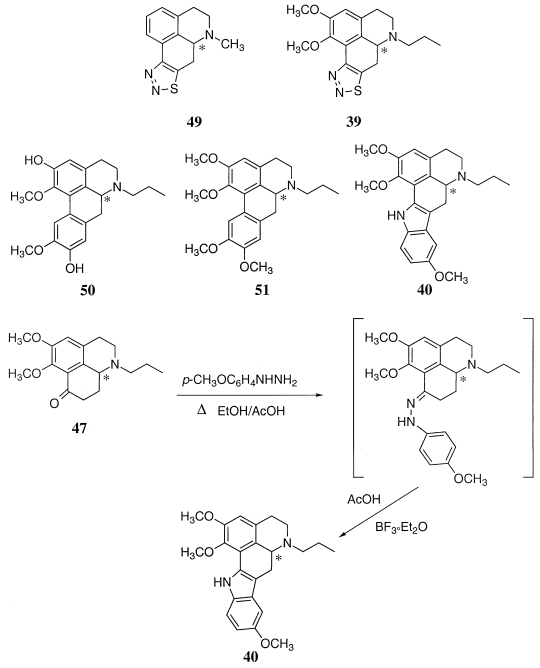

Scheme 2. Structures of **39**, **40**, **49**, **50** and **51** and the preparation of racemic **40**.

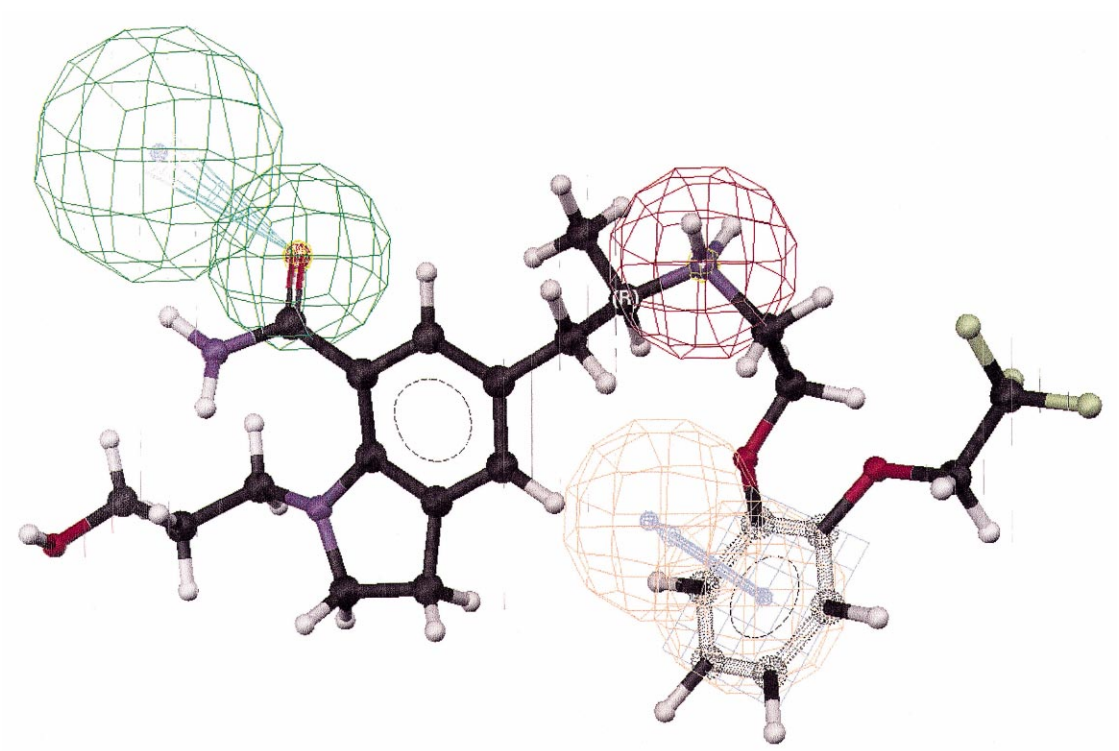

Figure 2. The α_{1A} pharmacophore based on Catalyst with KMD-3213 **16** mapped onto it. The molecule is shown with the chemical bonds represented as tubes and atoms colour coded according to the element type (black-C, white-H, red-O, blue-N, green-F). Mesh spheres represent the location constraints for the feature on the ligand (or receptor) and are colour coded according to feature: red - positive ion, green–hydrogen bond acceptor (the second, larger sphere relates to the position of the interacting group on the receptor), light brown - aromatic ring system (the second, larger sphere relates to the position of the interacting aromatic system on the receptor; the light blue square denotes the position of the plane of the aromatic system).

Table 2. Binding data for **39**, **40** and the aporphines **50** and **51** at the cloned and expressed human α_1-ARs

No.	Compound name	Activity (nM)		
		α_{1A}	α_{1B}	α_{1D}
39	Thiadiazole	50 000	126 000	31 600
40	IQC	4	250	100
50	Boldine	4.9[a]	320[a]	—
51	Glaucine	75[a]	1200[a]	—

[a]Ref. 27.

yield. Cyclisation of **46** to **47** was completed using oleum as the cyclising agent. Conversion of the amino ketone **47** to the semicarbazone **48** proceeded in good yield, however, reaction of **48** with thionyl chloride gave the required **39** in only 14% yield. The yield was very low in comparison to that reported[33] for the related derivative **49** (Scheme 2). The lower yield may possibly be due to side reactions involving the methoxy groups.

The amino ketone **47** could also be converted into the racemic ring D indole analogue IQC **40** via the non-isolated *p*-methoxyphenylhydrazone and subsequent Fischer indolisation using glacial acetic acid and BF_3-etherate (Scheme 2). The heterocyclic skeleton had been synthesised[34] previously by this general method but with dry hydrogen chloride as the acid catalyst. Structural confirmation of **39** and **40** was forthcoming from the NMR and MS data.

Receptor binding results

The ring D thiadiazole analogue **39** of the aporphine system, which was designed from the Apex-3D pharmacophore models, was tested on the cloned and expressed human α_{1A}, α_{1B} and α_{1D} receptors (Table 2). As can be seen, compound **39** had very low affinity for the α_1-ARs. In contrast, the ring D indole analogue, **40**, showed high affinity for these receptor subtypes, comparable to those of the aporphines **50** and **51**.

Molecular electrostatic potential (MEP) mapping

Electrostatic forces play an important role in determining the essential stereoelectronic features of biomolecules and drugs for QSAR studies. They also play an important role in determining the orientations of the molecules when approaching their receptors because of their long-range action compared to other intermolecular interactions. Both these effects are represented in charge distributions calculated by ab initio methods, which is the best source of information about the electrostatic properties of a molecule.

Models of the compounds **39**, **40** and **50** were built, optimised using ab initio calculations and the electrostatic potentials were then mapped onto the total electron density surfaces. This showed clearly that the differences between **39** and **40** or **50** lay in the electron density pattern located on the lower ring system which is the thiadiazole ring for **39**, the dimethoxybenzene ring for **50** and the methoxy-indole ring for **40** (see Scheme 2). Compound **39** had a negative potential section situated on the nitrogen atom, whereas the other two aporphine analogues, **50** and **40**, had an area of positive potential situated at the corresponding part of the lower aromatic ring. This electron rich edge of **39** could cause an unfavourable interaction with the receptor, and hence possibly explain the poor affinity of **39** for α_1 ARs.

Further pharmacophore development

In the light of these experimental results and the possibility of distinct and different binding sites for several important classes of α_1 AR antagonists, further pharmacophore development was deemed necessary, before the design of new, potentially selective ligands could be attempted.

Catalyst treats molecular structures as templates consisting of strategically positioned chemical functions that will bind to a receptor. Molecular flexibility is taken into account by considering each compound as a collection of conformers representing different areas of conformational space available to the molecule within a given energy range.[35] The structures of known subtype selective AR antagonists used in this study are shown in Figure 1 and their binding affinities and selectivities

Table 3. Experimental activity and estimated activities of the compounds of Table 1 and Figure 1 for the α_{1A} hypothesis

No.	Compound name	Activity (nM)	
		Measured	Estimated
1	Prazosin	0.2	2.8
2	Cyclazosin	12	2.8
3	Abanoquil	0.04	2.8
4	REC-15/2615	1.9	2.8
5	Alfuzosin	10	2.9
6	Doxazosin	3.16	2.8
7	Terazosin	6.3	2.8
8	Bunazosin	0.5	2.8
9	(+)-Niguldipine	0.15	0.16
10	SNAP-5089	0.23	2.8
11	SNAP-5399	0.65	0.49
12	SNAP-5150	1.9	0.086
13	WB-4101	0.16	0.3
14	Phentolamine	1.6	2.8
15	5-Methyluropidil	0.63	0.59
16	KMD-3213	0.04	0.039
17	AH-11110A	2500	2.8
18	BMY-7378	250	2.9
19	SKF-104856	44	6.3
20	Discretamine	616	5.7
21	Corynanthine	142	2.1
22	Benzoxathian	0.2	0.85
23	Spiperone	7.9	2.9
24	(+)-YM-617	4.3	0.31
25	SNAP-8719	294	2.9
26	Indoramin	4.0	0.17
27	RS-17053	0.6	0.88
28	A-131701	0.22	0.058
29	NAN-190	2.0	0.22
30	WAY-100635	144	0.43
31	RS-100,975	1.0	1.2
32	REC-15/2739	1.0	0.11
33	SNAP-1069	16	0.22
34	SL-89.0591	2.5	0.61
35	JHT-601	0.4	2.8
36	GG-818	0.2	0.18
37	Uropidil	288	1.1
38	Bromotopsentin	12000	0.58

tabulated in Table 1. The compounds are grouped together according to structural features, so that the quinazolines **1**–**8** are listed first, followed by the niguldipine analogues **9**–**12** and other antagonists.

In an attempt to generate general α_1 subtype pharmacophores, applicable to all structural classes of ligands, the complete training set of 38 antagonists was selected. Protonated forms of the antagonists were built to predefine at least this one common feature between all molecules, as this is postulated to be an essential feature for α_1 AR ligand binding (see Introduction). Conformational searching was performed using a 20 kcal/mol energy threshold with respect to the global energy minimum. The Catalyst software uses molecular mechanics (force field) calculations[36] and a particular way to handle the conformational space (poling method).[37,38] The compounds in the training set and their associated conformational models were submitted to generate hypotheses for general α_1 models. The chemical features used in this generation step included positive ion, hydrogen bond acceptor and donor, aromatic ring and hydrophobic groups. The aromatic ring function also allows consideration of the directionality of π–π interactions and constrains the plane of the aromatic system. Catalyst provides two numbers to assess the validity of a pharmacophore (hypothesis):

1. The cost of an ideal hypothesis which is a lower bound on the cost of the simplest possible hypothesis that still fits the data perfectly.
2. The cost of the null hypothesis which assumes that there is no statistically significant structure in the data and that the experimental activities are normally distributed about their mean.

According to the assessment criteria, a generated hypothesis with a score that is substantially below the cost of the null hypothesis, is likely to be statistically significant.

The program gives 10 of these hypotheses as a result of an experiment by default. Sometimes however, the first of these is empty so that only nine hypotheses are obtained, which are numbered 2–10. Activity data for each of the three subtypes was also included in the input of these three experiments. However, the resulting hypotheses, which included the positive ion feature, had several problems. The correlations between the predicted and experimental affinities were fairly low for the compounds of the training sets (0.76 for α_{1A}, 0.84 for α_{1B}, 0.82 for α_{1D}). Of special concern in this respect was the fact that high errors (>5-fold) were observed for the binding affinity estimation of compounds selective for the subtype under consideration (niguldipine (**9**), SNAP 5089 (**10**), Me-uropidil (**15**), KMD-3213 (**16**), RS-100,975 (**31**) and GG-818 (**36**) for the α_{1A} subtype; AH-11110A (**17**), spiperone (**23**), and bromotopsentin (**38**) for the α_{1B} subtype; SKF-104856 (**19**), SNAP-8719 (**25**), and NAN-190 (**29**) for the α_{1D} subtype). Furthermore, the ring aromatic feature was not present in the α_{1A} top hypothesis, but only the less specific hydrophobic feature, which, with the exception of the quinazolines, is not usually mapped onto an aromatic ring system. The same is true for the aromatic ring feature which is present in the α_{1B} pharmacophore hypothesis.

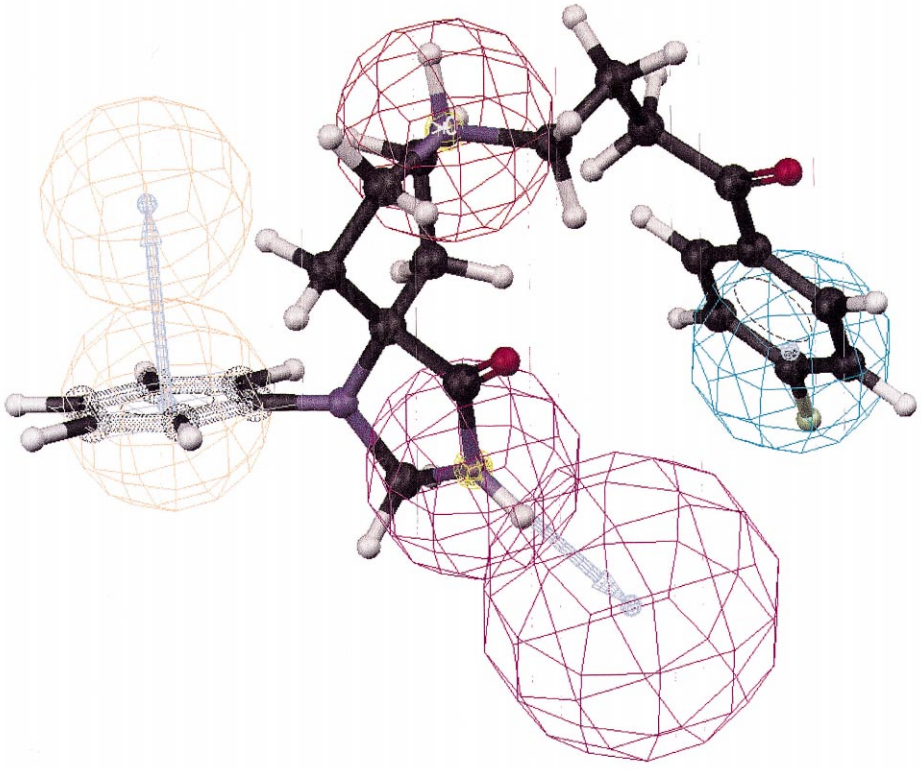

Figure 3. The α_{1B} pharmacophore based on Catalyst with spiperone **23**. See Figure 2 for explanation of symbols. Additionally, this pharmacophore contains a hydrogen bond donor feature (purple spheres) and a hydrophobic group (blue sphere).

For the α_{1D} hypothesis, the situation was slightly different, in that the positive charge feature and the aromatic ring feature were mapped together in 14 out of the 37 training set compounds, however, in nine compounds the positive charge feature was not mapped. These findings confirm previous observations,[25,30,31] suggesting that not all the compounds in Table 1 share the same binding sites at the α_1 ARs. We also found that these 'inclusive' pharmacophore models were not very successful in predicting the affinity of our lead compound, IQC **40** (prediction errors were nine fold for α_{1A}, 18-fold for α_{1B}, and 67-fold for α_{1D}).

We thus decided to pursue this further by constructing new models with training sets excluding both the niguldipine analogues and the quinazolines and also with training sets excluding only one of those two classes of compounds. Upon taking the quinazolines (and close analogues) **1**–**8** out of the training set, the correlation between predicted and experimental affinities for the training set molecules did indeed improve, as did the mapping of aromatic ring systems together with the positive charge feature and the accuracy of the predictions for IQC **40**. These pharmacophore models still did not predict highly selective compounds in the training set very well. On the other hand, removing the niguldipines **9**–**12** (the inclusive term niguldipines is used for simplicity) from the training sets did not have a large effect on the pharmacophores. For example, for the α_{1A} model, the aromatic ring feature was still not included in this case. Also, taking out both the niguldipine analogues and the quinazolines from the training sets, did not improve the pharmacophore models significantly compared to the ones when only the quinazolines were removed. Because we were mainly interested in the features responsible for selectivity between α_1 AR subtypes, we decided to construct pharmacophore models based on training sets containing only α_1 receptor subtype selective compounds, but also excluding quinazoline derivatives and close analogues (because our results above confirmed our previous suspicion[25] that these interact with α_1 ARs in a different way), and niguldipines. These pharmacophore models are discussed below. Since the training sets used for their derivation were now small, these hypotheses serve only as possible qualitative models.

α_{1A} Pharmacophore model

Only antagonists **15**, **16**, **31** and **36** which had some selectivity for the α_{1A} subtype over the other subtypes, were used in the training set (required selectivities were 50-fold over α_{1B} and 10-fold over α_{1D}). The chemical functions used in the hypothesis generation step were the same as above. Nine hypotheses were obtained by default. Even though hypothesis 3 had a slightly higher cost than hypothesis 2, this former hypothesis was chosen as the best model due to the existence of a positive ion feature. The best hypothesis (Fig. 2) consisted of three features including a positive charge in the middle of the system, a hydrogen bond acceptor group and an aromatic ring system at opposite ends of the molecules. This hypothesis had a very good correlation between the experimental affinities and the estimated values for the training set (1.0). The error in predicting IQC **40** is 1.4-fold. As with our previous Apex-3D pharmacophores,[25] the predictions for the affinities of **39** and **40** are very similar and indicate the fundamental failing of pharmacophore models in not taking detrimental electrostatic effects into account as discussed earlier. The hypothesis was also used to predict the affinities for all compounds in Table 1 and the results are shown in Table 3. Overall, the correlation (0.35) with the experimental values was still not good but, interestingly, most of the poor predictions were for compounds which exhibit weak α_{1A} affinity (all eight compounds with $K_i > 100$ nM are predicted very poorly). Prazosin and abanoquil are also very poorly predicted, whereas the other quinazolines are predicted reasonably well. The same is true for the niguldipines, where SNAP-5150 and SNAP-5089 are not predicted well, whereas the other two members of this group are predicted very well.

α_{1B} Pharmacophore model

Only three antagonists (**17**, **23** and **38**) were used in the training set of this experiment. These compounds display at least 10-fold selectivity over the α_{1A} subtype, and

Table 4. Experimental activity and estimated activites of the compounds of Table 1 and Figure 1 for the α_{1B} hypothesis

No.	Compound name	Activity (nM)	
		Measured	Estimated
1	Prazosin	0.25	160
2	Cyclazosin	0.13	280
3	Abanoquil	0.08	250
4	REC-15/2615	0.3	190
5	Alfuzosin	10	220
6	Doxazosin	1.0	350
7	Terazosin	2.0	190
8	Bunazosin	1.0	190
9	(+)-Niguldipine	55	290
10	SNAP-5089	13	690
11	SNAP-5399	324	610
12	SNAP-5150	331	270
13	WB-4101	2.5	360
14	Phentolamine	7.9	870
15	5-Methyluropidil	40	600
16	KMD-3213	20	150
17	AH-11110A	76	79
18	BMY-7378	630	1800
19	SKF-104856	63	660
20	Discretamine	360	5500
21	Corynanthine	517	550
22	Benzoxathian	4.0	270
23	Spiperone	0.5	0.52
24	(+)-YM-617	96	110
25	SNAP-8719	191	2400
26	Indoramin	40	100
27	RS-17053	16	140
28	A-131701	6.95	150
29	NAN-190	15	1700
30	WAY-100635	186	930
31	RS-100,975	479	140
32	REC-15/2739	32	160
33	SNAP-1069	200	160
34	SL-89.0591	13	88
35	JHT-601	1.2	650
36	GG-818	16	150
37	Uropidil	1320	380
38	Bromotopsentin	740	750

additionally quinazolines (cyclazosin) and niguldipines were excluded. The same chemical features were used in the generation step. Nine hypotheses were obtained and hypothesis 2 (lowest cost hypothesis) was chosen as the best hypothesis because it also contained a positive charge and an aromatic ring feature. This hypothesis consisted of four features including a hydrogen bond donor group and a hydrophobic group as well as the aromatic ring system and the positive charge (see Fig. 3). This hypothesis showed a very good correlation (1.00) between the experimental activity and the estimated values for the training set. All compounds in Table 1 were estimated with this hypothesis and the results are shown in Table 4. The overall correlation is 0.37. In this case, all quinazolines are predicted very poorly with errors of 20-fold and greater. Two of the niguldipines are predicted quite well, but they possess relatively poor affinity for the α_{1B} site. This is a general problem with this hypothesis. It underestimates (error >5) the affinity of 23 out of the 28 compounds with high affinity (K_i < 100 nM). The aporphine derived compounds **39** and **40** are correctly predicted to have much lower affinity at α_{1B} than for the α_{1A} subsite (K_i = 780 nM for **40**, error is 3-fold, K_i = 5300 nM for **39**).

α_{1D} Pharmacophore model

Only four compounds in Table 1 show at least 10-fold selectivity over the α_{1A} receptor subtype. Of these, BMY-7378 and SNAP-8719 are structurally very similar (see Fig. 1). Including both would have distorted the training set, so only three compounds (**19**, **20** and **25**) were used. Quinazolines and niguldipines were again excluded. Nine hypotheses were generated, but the first three did not contain a positive ion feature and none of them contained an aromatic ring feature as well as a positive ion feature. Hypothesis 5 was selected, as it was the lowest cost hypothesis to contain a positive ion. It also includes a hydrophobic group and a hydrogen bond acceptor and is shown in Figure 4 with SNAP-8719 mapped onto it. For both discretamine and SNAP-8719 the hydrophobic feature is in fact mapped onto an aromatic ring, but SKF-104856 has only one phenyl ring which is much closer to the positively charged nitrogen. The correlation between estimated and experimental affinities for the training set molecules is excellent (1.00). Again, we have compared all molecules in Table 1 with this hypothesis and the results are tabulated in Table 5. The correlation is −0.14 (no correlation). This hypothesis underestimates the affinity of all quinazolines, whereas all niguldipines are overestimated. The remainder of the compounds are under- or overestimated with equal frequency. Our lead compounds (**39** and **40**) are again estimated to have very similar affinities (58 versus 77 nM for the K_i values of (**39** and **40**); error for **40** is 1.3-fold).

Discussion

We have shown that it is not possible to construct pharmacophores for the binding of antagonists to α_1 receptor subtypes that are valid for all structural classes of antagonists in Table 1 and Figure 1. The relative positions of the protonated nitrogen atom and the aromatic systems are different, especially for the quinazolines, and the quality of the pharmacophore improves when these compounds are excluded from the training sets. From these results it is quite likely that these ligands, which generally exhibit very high affinity for all

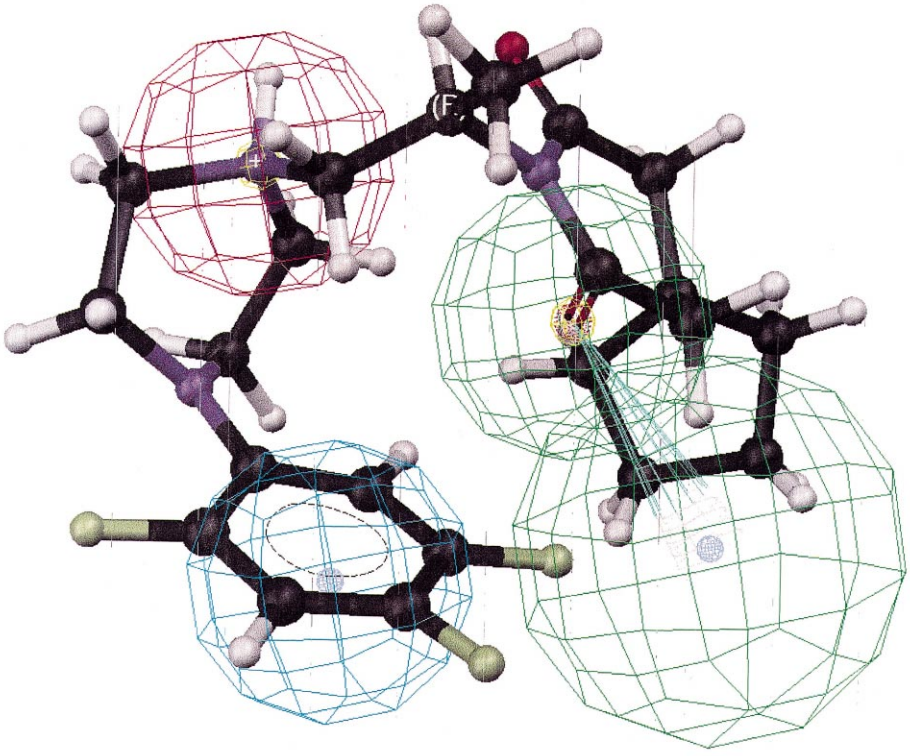

Figure 4. The α_{1D}-pharmacophore with SNAP-8719 **25**. See Figures 2 and 3 for explanation of symbols.

Table 5. Experimental activity and estimated activites of the compounds of Table 1 and Figure 1 for the α_{1D} hypothesis

No.	Compound name	Activity (nM)	
		Measured	Estimated
1	Prazosin	0.32	6.7
2	Cyclazosin	3.2	9.1
3	Abanoquil	0.04	8.1
4	REC-15/2615	2.6	8.6
5	Alfuzosin	3.16	5.8
6	Doxazosin	4	7.5
7	Terazosin	2.5	8.5
8	Bunazosin	1	7.3
9	(+)-Niguldipine	100	2.6
10	SNAP-5089	66	3.2
11	SNAP-5399	631	2.7
12	SNAP-5150	400	3.9
13	WB-4101	0.25	4.8
14	Phentolamine	7.9	20
15	5-Methyluropidil	10	18
16	KMD-3213	2	2.3
17	AH-11110A	2750	5.4
18	BMY-7378	6.3	2.2
19	SKF-104856	5.2	4.8
20	Discretamine	25	24
21	Corynanthine	253	5.8
22	Benzoxathian	0.4	5
23	Spiperone	13	4.5
24	(+)-YM-617	22	4.1
25	SNAP-8719	1.6	1.8
26	Indoramin	160	4.7
27	RS-17053	16	3.9
28	A-131701	0.97	4.9
29	NAN-190	0.8	7.5
30	WAY-100635	63	3.2
31	RS-100,975	100	3.5
32	REC-15/2739	2.5	2.5
33	SNAP-1069	790	3.4
34	SL-89.0591	2.5	12
35	JHT-601	1.2	7.5
36	GG-818	25	10
37	Uropidil	1660	11

three α_1 AR subtypes, but little subtype selectivity, bind to a different site, common to all α_1 ARs.

Our results are, however, not as definitive in this respect for the niguldipines, a class of compounds exhibiting very high α_{1A} affinities and selectivities.

For all these 'inclusive' pharmacophores, the additional variable of the selectivity between the α_1 AR subtypes was not considered. Table 1 contains compounds with high affinity, but low selectivity (e.g. prazosin (**1**)) and compounds with low affinity, but high selectivity (e.g. bromotopsentin (**38**)). The Catalyst program, having only received information about the affinity, discriminates against compounds such as bromotopsentin in favour of compounds such as prazosin. This was reflected in the fact that all these "inclusive" pharmacophores predict the affinity of selective antagonists very poorly, and this was also true for the predictions of our lead compounds **39** and **40**. Since we were primarily interested in the design of new subtype selective ligands based upon our aporphine type lead compounds, we decided to employ a different approach towards pharmacophore development.

This consisted of restricting the training sets for the pharmacophores severely by only including selective ligands which were neither quinazolines, nor niguldipines, and these are the pharmacophores presented in Figures 2–4.

All three α_1 AR subtype pharmacophores so constructed predict IQC **40** very well and can therefore be considered useful for the further design of more selective ligands based on that compound (see below). They all, however, also predict the 1,2,3-thiadiazole derivative **39** to exhibit very similar affinities to **40**, contrary to the experimental findings (see Table 2). This can be explained by the fact that the software is not able to take detrimental electrostatic effects into account.

These pharmacophore models are only to be considered as qualitative models, however, as can be seen from their generally poor predictive abilities for the compounds of Table 1.

Comparison of the pharmacophore models and implications for ligand design

In Figure 5 the three subtype specific α_1 pharmacophore models derived solely from selective ligands are compared. All three contain a protonated nitrogen atom, and while this contributes to the affinity of each compound, in terms of selectivity it would be desirable to design a ligand not containing such a feature. For this ligand to exhibit enough affinity it would however be necessary to start with a pharmacophore of at least three other features (which in our case is only possible for the α_{1B} subtype) and a lead compound with high affinity for this subtype. A feature unique to the pharmacophore for ligands at the α_{1B} subtype is a hydrogen bond donor (HBD) group. For the α_{1A} pharmacophore, there is a hydrogen bond acceptor group (HBA), located much further away from the positive ion (see Table 6 for the distances and angles between the features for the three pharmacophores), and for the α_{1D} pharmacophore, the equivalent distance is smaller. When mapping IQC **39** onto the α_{1B} pharmacophore, the HBD feature is not mapped, but it is close to the indole nitrogen. We have, furthermore, observed a hydrogen bonding interaction between this indole NH of IQC and the α_{1B} receptor, when docking the ligand into the computer model of the transmembrane helices of the receptor.[39] Additionally, this NH group, incorporated into the indole ring, is not considered to be an HBA within the Catalyst software and thus cannot be mapped onto the HBA feature of the α_{1A} and α_{1D} pharmacophores. A ligand selective for the α_{1B} over the other two α_1 AR subtypes might thus be achieved by replacing the *O*-methyl groups in **2** with alkyl groups, to provide hydrophobic interactions and avoid any HBA capability. This compound would be able to interact with all four features of the α_{1B} pharmacophore, leading to a predicted affinity in the same order of magnitude as that for IQC **2** (250 nM), whereas the affinity for the α_{1A} and α_{1D} subtypes should be reduced by two orders of magnitude to around 400 and 10,000 nM, respectively. As was predicted by the original Apex 3D pharmacophores,

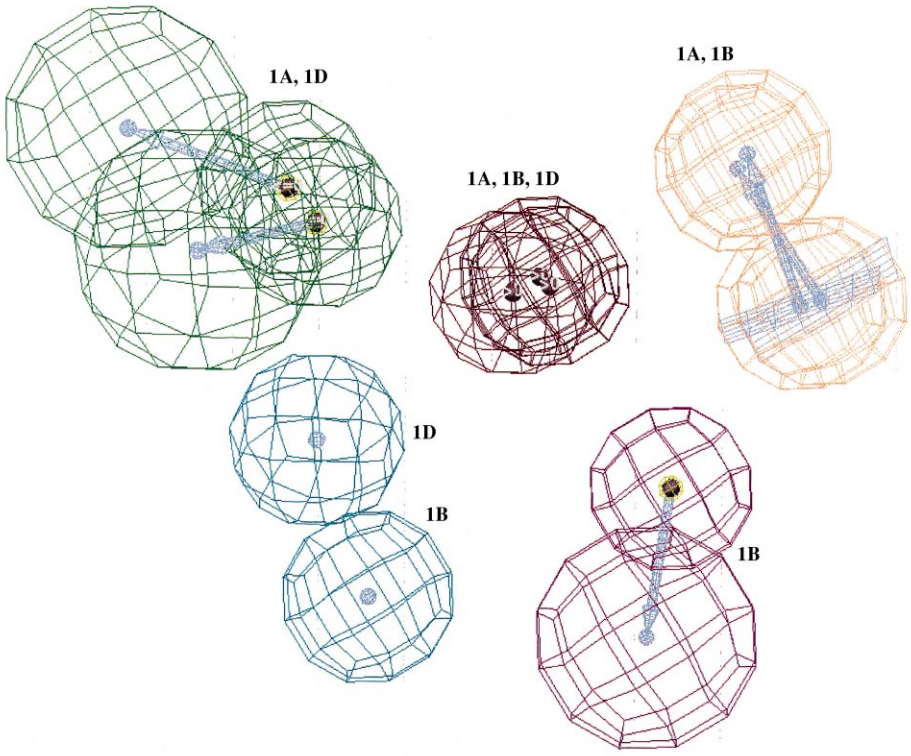

Figure 5. Overlap of the three pharmacophores. Letters indicate the subtype to which the feature belongs.

Table 6. Distances and angles between pharmacophore features

Pharmacophore model	Distances (Å) and angles (°) between features[a]
α_{1A}	P - A 5.5; P - HBA 7.1; A - P - HBA 100
α_{1B}	P - A 6.2; P - H 7.8; P - HBD 4.9; H - P - HBD 57; A - P - HBD 52
α_{1D}	P - H 5.4; P - HBA 4.5; H - P - HBA 47

[a]Abbreviations used for features: P, positive charge; HBA, hydrogen bond acceptor; A, aromatic ring centre; H, hydrophobic group; HBD, hydrogen bond donor.

although true to a lesser extent, the distance between the aromatic feature and the positive charge is smaller for the α_{1A} subtype and selectivity for α_{1B} may be further improved by separating the indole and the tetrahydroisoquinoline aromatic systems by a larger ring and/or removing the aromatic portion of the tetrahydroisoquinoline system altogether. The former modification would also potentially strengthen a weak, long aromatic interaction observed for the indole phenyl ring in our docking experiments.[39]

Conclusion

Pharmacophores for selective antagonists at the α_{1A} and α_{1B} adrenoceptor sites were developed together with a preliminary antagonist pharmacophore for the α_{1D} adrenoceptor, which is the first pharmacophore reported for this particular subtype. These pharmacophores should be useful for designing ligands based on the aporphine skeleton, as long as suitable care is taken not to introduce unfavourable electrostatic effects. The importance of this was shown with **39**, which, despite predictions, showed very low α_1 affinities. The fact that molecular fields in general, and electrostatic potentials in particular, are not considered in the pharmacophore development is an important limitation of this approach and has been highlighted again here. The Catalyst software does allow the placement of excluded volume features, the location of which can be determined using receptor models (in the absence of any experimental 3D structure of any adrenoceptor) and this is currently under investigation.

Experimental

Synthesis

All melting points were determined using a Reichert hot stage melting point apparatus and are uncorrected. The ^{1}H nuclear magnetic resonance spectra (NMR) were determined at 300 or 400 MHz with a Varian Unity-300 or -400 spectrometer. The ^{13}C NMR spectra were recorded using the same instruments at 75 or 100 MHz. Unless otherwise stated, the spectra were obtained on solutions in $CDCl_3$ and referenced to TMS. The electron impact (EI) mass spectra were obtained on a Shimadzu QP-5000 mass spectrometer using the direct insertion technique, with an electron beam energy of 70 eV and a source temperature of 260 °C. The peak intensities, in parentheses, are expressed as a percentage abundance. For the chemical ionisation (CI) mass spectra, isobutane was used as the ionising gas in a Shimadzu QP-5000 mass spectrometer. The low resolution electrospray mass spectra were obtained on a Vacuum General Quattro mass spectrometer using 50% aqueous

acetonitrile as solvent and a skimmer cone voltage of 25 V. Where electrospray MS data is reported, it refers to the positive ion mode. The high resolution mass spectra (HRMS) were obtained using either a Vacuum General Autospec-OA-TOF mass spectrometer using the same conditions as for the Quattro mass spectrometer and a resolution of 5000 or a Vacuum General Micromass 7070F spectrometer employing the direct insertion technique, with an electron beam energy of 70 eV and a source temperature of 200 °C. Analytical thin layer chromatography (TLC) was performed on Merck Kieselgel 60PF_{254} silica on plastic backed sheets. R_f values were recorded from the centre of the spots. All chromatographic solvent proportions are volume by volume. Column chromatography was performed using Merck silica gel (mesh size = 0.032–0.064 mm) under medium pressure. All reagents and solvents were purified and dried by standard techniques.[40] The drying of chloroform, diethyl ether or dichloromethane extracts was done with anhydrous magnesium sulfate or sodium sulfate. Solvents were removed under reduced pressure in a rotary evaporator. Light petroleum used had a boiling point range of 40–60 °C.

Micro analyses were carried out on a Carlo Erba, CHNS-O EA1108 Elemental Analyser in the Central Science Laboratory, University of Tasmania.

Preparation of 6,7-dimethoxy-1-methyl-3,4-dihydroisoquinoline (41). To a stirred mixture of 2-(3,4-dimethoxyphenyl)ethylamine (30.09 g, 145 mmol) and dry pyridine (15 mL; distilled over potassium hydroxide) under nitrogen was added acetic anhydride (19 mL) dropwise to maintain a reaction temperature of 60–70 °C. The temperature was then increased to 90 °C for 1 h. The solution was left at room temperature overnight. Pyridine and acetic acid were distilled and the crude 2-[(3,4-dimethoxyphenyl)ethyl]ethanamide recrystallised from ethyl acetate to afford colourless crystals (23.81 g, 107 mmol, 79%); m.p. 98–100 °C. MS (EI): *m/z* 223 ($M^{+\cdot}$, 100%). HRMS: *m/z* 223 (M^+, 28%, accurate mass 223.119. $C_{12}H_{17}NO_3$ requires 223.121). ^{1}H NMR δ: 6.822 (d, J = 8.3 Hz, 1H, ArH); 6.753 (s, 1H, ArH); 6.732 (d, J = 7.5 Hz, 1H, ArH); 3.876 (s, 6H, 2×Ar-OCH_3); 3.503 (q, J = 6.6 Hz, 2H, H-2′); 2.773 (d, J = 6.9 Hz, 2H, H-1′); 1.952 (s, 3H, CH_3); 5.560 (s, NH). ^{13}C NMR δ: 169.9 (C=O), 148.8 (C-3), 147.5 (C-4), 131.2 (C-1), 120.4, 111.7, 111.2 (C-2, C-5, C-6), 55.7 (2×Ar-OCH_3), 40.6 (C-2′), 35.0 (C-1′), 23.1 (CH_3).

To a mixture of dry toluene (90 mL) and 2-[(3,4-dimethoxyphenyl)ethyl]ethanamide (15.4 g, 69 mmol), at 60 °C, freshly distilled phosphoryl chloride (18 mL) was added dropwise over 30 min. The mixture was refluxed until hydrogen chloride evolution ceased (2.5 h), and then was cooled on ice. The toluene was decanted and the crystals washed with light petroleum containing a few drops of toluene. The crystals were dissolved in water (50 mL) and the solution cooled on ice. Basification to pH 11 of the mixture with 32% sodium hydroxide (50 mL) was undertaken with ice added to maintain a reaction temperature below 30 °C. The product was extracted with portions of dichloromethane (3×20 mL) which were combined, washed with water (5 mL) and dried. The product was collected after evaporation as a yellow powder (10.86 g, 53 mmol, 76%), which yielded **41** as colourless crystals after recrystallisation from diethyl ether; m.p. 98–100 °C (Found: C, 70.0; H, 7.5; N, 7.0%. $C_{12}H_{15}NO_2$ requires C, 70.2; H, 7.4; N, 6.8%. MS (EI): *m/z* 205 (M^+, 100%), 190 (55), 174 (15), 160 (12), 147 (10), 131 (8). HRMS: *m/z* 205 (M^+, 100%, accurate mass 205.110. $C_{12}H_{15}NO_2$ requires 205.110). ^{1}H NMR δ: 6.991 (s, 1H, ArH); 6.694 (s, 1H, ArH); 3.923 (s, 6H, 2×Ar-OCH_3); 3.662 (t, J = 7.6 Hz, 2H, H3); 2.636 (t, J = 7.6 Hz, 2H, H4); 2.372 (s, 3H, C-1′). ^{13}C NMR δ: 163.4 (C-1), 150.6, 147.2 (C-6, C-7), 130.9 (C-8a), 122.3 (C-4a), 110.0, 108.8 (C5, C8), 56.0, 55.8 (2×Ar-OCH_3), 46.8 (C-3), 25.6 (C-4), 23.2 (C-1′).

Preparation of 6,7-dimethoxy-1-methyl-2-propyl-3,4-dihydroisoquinolinium iodide (42). Excess 1-iodopropane (1.6 mL; freshly distilled over anhydrous potassium carbonate) and the finely powdered **41** (1.86 g, 9 mmol) were placed in a sealed tube. This mixture was heated at 90 °C for 24 h. The solid was removed from the tube with a small amount of dichloromethane and diethyl ether was added to recrystallise the crude product. This was filtered and washed with diethyl ether to give **42** (2.85 g, 7.6 mmol, 84%) as a pale yellow powder; m.p. 179–180 °C. Found: C, 47.7; H, 5.9; N, 3.8. $C_{15}H_{21}NO_2$ requires C, 48.0; H, 5.9; N, 3.7%. MS (ES): *m/z* 247 (375-HI, 45%), 232 (30), 216 (9), 205 (97), 190 (49), 174 (18), 160 (12), 142 (100). HRMS: *m/z* 247 (M-HI^+, 79%, accurate mass 247.159. $C_{15}H_{21}NO_2$ requires 247.157). ^{1}H NMR δ: 7.282 (s, 1H, ArH); 6.917 (s, 1H, ArH); 4.112 (t, J = 7.6 Hz, 4H, $2CH_2$); 4.013, 3.916 (s, 6H, 2×Ar-OCH_3); 3.253 (t, J = 7.7 Hz, 2H, H4); 3.032 (s, 3H, CH_3); 1.987–1.903 (m, 2H, H-2′); 1.092 (t, J = 7.4 Hz, 3H, CH_3). ^{13}C NMR δ: 173.7 (C-1); 156.3, 148.6 (C-6, C-7); 137.8 (C-8a); 119.7 (C-4a); 112.4, 110.6 (C-5, C-8); 59.2 (C-3); 56.9, 56.8 (2×Ar-OCH_3); 51.1 (C-1′); 26.1 (C-4), 21.2 (C-2′); 20.3 (CH_3); 11.1 (C-3′).

Preparation of 6,7-dimethoxy-1-methylidene-2-propyl-1,2,3,4-tetrahydroisoquinoline (43). A solution of **42** (16.75 g, 45 mmol) in water (50 mL) was basified with 32% sodium hydroxide. This mixture was then extracted rapidly with portions of diethyl ether (3×20 mL), the extracts combined, dried and the solvent evaporated to give crude **43** (9.79 g, 40 mmol, 89%) as a yellow–orange syrup. MS (EI): *m/z* 247 ($M^{+\cdot}$, 45%), 232 (30), 219 (8), 205 (100), 190 (45), 174 (15), 160 (10), 142 (8). HRMS: *m/z* 247 (M^+, 69%, accurate mass 247.257. $C_{15}H_{21}NO_2$ requires 247.257). ^{1}H NMR δ: 7.203 (s, 1H, ArH); 6.573 (s, 1H, ArH); 4.30 (bs, integrated less than 2H, C-1′); 3.90 (s, 3H, Ar-OCH_3); 3.84 (s, 3H, Ar-OCH_3); 3.23–3.18 (m, 4H, $2CH_2$); 2.80 (t, J = 5.9 Hz, 2H, H4); 1.73–1.60 (m, 2H, C-2′); 0.94 (t, J = 7.4 Hz, 3H, C-3′). ^{13}C NMR δ: 148.5 (C-1), 147.2, 146.2 (C-6, C-7), 127.5 (C-8a), 124.8 (C-4a), 110.2, 107.9 (C-5, C-8), 75.3 (C-1′), 55.7, 55.5 (2×Ar-OCH_3), 54.0 (C-3), 47.7 (C1′), 29.8 (C-4), 18.6 (C-2′), 11.5 (C-3′).

Preparation of 1-[2-(ethoxycarbonyl)ethyl]-6,7-dimethoxy-2-propyl-3,4-dihydroisoquinolinium bromide (44). To the crude enamine (**43**) (9.79 g, 40 mmol), at 0 °C and under

nitrogen gas, ethyl bromoacetate (40 mL) was added dropwise with stirring. The solution was then heated to 60 °C for 30 min. Dry toluene was added and the product was collected as cream crystals (13.64 g, 33 mmol, 83%). Recrystallisation from dry ethanol/diethyl ether afforded pure **44** as a yellow powder; m.p. 176–178 °C. Found C, 54.8; H, 7.2; N, 3.63. $C_{19}H_{28}BrNO_4$ requires C, 55.1; H, 6.8; N, 3.4%. MS (ES): *m/z* 334 (M-Br, 100%). HRMS: *m/z* 333 (M-HBr$^+$, 27%, accurate mass 333.195. $C_{19}H_{27}NO_4$ requires 333.194). ^{1}H NMR δ: 7.502 (s, ArH); 6.963 (s, ArH); 4.262–4.059 (m, 3CH_2); 4.011 (s, OCH_3); 4.098 (s, OCH_3); 3.752 (t, J = 7.7 Hz, H4); 3.235 (t, J = 7.5 Hz, H-3); 2.942 (t, J = 7.1 Hz, CH_2); 2.097–1.924 (m, 2H, CH_2); 1.223 (t, J = 7.1 Hz, CH_3); 1.097 (t, J = 7.4 Hz, CH_3). ^{13}C NMR δ: 176.0 (C=O), 171.2 (C-1), 156.3, 148.4 (C-6, C-7), 133.7 (C-8a), 118.1 (C-4a), 112.6, 110.8 (C-5, C-8), 61.4 (C-3), 59.2 (C-4″), 57.1, 56.7 (2×Ar-OCH_3), 51.5 (C-1′), 32.7 (C-2″), 26.4 (C-4), 26.0 (C-1″), 21.6 (C2′), 14.0 (C-5″), 11.1 (C-3').

Preparation of ethyl 3-[6,7-dimethoxy-2-propyl-1,2,3,4-tetrahydro-isoquinolin-1-yl]-propanoate (45). To a stirred solution of **44** (2.00 g, 4.8 mmol) in ethanol (15 mL) at 0 °C, was added sodium borohydride (0.42 g) over 1 h. The reaction mixture was left overnight at room temperature. The ethanol was then evaporated and the residue dissolved in water (4 mL). The solution was extracted with portions of diethyl ether (3×10 mL) which were combined, dried and the solvent evaporated leaving a clear, pale green syrup (1.54 g, 4.6 mmol, 95%). This was purified by medium pressure column chromatography to yield pure **45** as a colourless syrup. MS (ES): *m/z* 336 (MH$^+$, 100%). HRMS: *m/z* 334 (M-H$^+$, 3%, accurate mass 334.200. $C_{19}H_{28}NO_4$ requires 334.202). ^{1}H NMR δ: 6.583 (s, 1H, ArH); 6.552 (s, 1H, ArH); 4.127 (q, J = 7.1 Hz, 2H, CH_2); 3.856 (s, 6H, 2OCH_3); 3.544 (t, J = 6.5 Hz, 1H, H-1); 3.156–3.108 (m, 1H); 2.801–2.744 (m, 2H); 2.543–2.402 (m, 5H); 2.033–1.949 (m, 2H); 1.535–1.462 (m, 2H, CH_2); 1.264 (t, J = 7.1 Hz, 3H, CH_3); 0.891 (t, J = 7.4 Hz, 3H, CH_3). ^{13}C NMR δ: 174.3 (C=O), 147.2 (C-6, C-7), 129.9 (C-8a), 126.7 (C-4a), 111.2, 110.5 (C-5, C-8), 63.1 (C-3), 62.5 (C-1), 60.0 (C-4″), 59.8 (C-1′), 55.9, 55.8 (2×Ar-OCH_3), 55.4 (C-11), 43.7 (C-4); 31.0 (C-2″), 23.7 (C-1″), 21.1 (C-2′), 14.2 (C-5″), 11.8 (C-3′).

Preparation of 1-[2-(carboxyethyl)]-6,7-dimethoxy-2-propyl-1,2,3,4-tetrahydroisoquinolinium chloride (46). The compound **45** (1.04 g, 3.10 mmol) was dissolved in 2 M hydrochloric acid (3 mL). This solution was stirred at room temperature under nitrogen gas and shielded from light for 4 days. The solvents were removed in vacuo over 24 h, the crude product collected as a white foam (0.96 g, 2.79 mmol, 90%). This was recrystallised from dry methanol/diethyl ether to yield pure **46** as a colourless powder; m.p. 168–170 °C. Found: C, 59.3; H, 7.7; N, 4.2. $C_{17}H_{26}ClNO_4$ requires C, 59.4; H, 7.6; N, 4.1%. MS (ES): *m/z* 308 (M-^{35}Cl, 1%), 292 (2), 249 (8). HRMS: *m/z* 306 (M-$H_2^{35}Cl^+$, 1%, accurate mass 306.171. $C_{17}H_{24}NO_4$ requires 306.170). ^{1}H NMR δ: 6.804 (s, 1H, ArH); 6.644 (s, 1H, ArH); 4.502 (t, 1H, H1); 3.891, 3.871 (s, 6H, OCH_3); 3.752 (m, 1H); 3.51 (m, 1H); 3.031 (m, 4H); 2.854 (m, 1H); 2.697 (m, 2H); 2.123–2.052 (m, 4H); 0.943 (t, J = 7.4 Hz, CH_3). ^{13}C NMR δ: 174.4 (C=O), 149.3, 149.1 (C-6, C-7), 122.0, 121.0 (C-8a, C-4a), 110.1, 110.8 (C-5, C-8), 67.6 (C-3), 64.3 (C-1), 61.7 (C-1′), 56.2, 55.9 (2×Ar-OCH_3), 42.2 (C-4), 30.8 (C-2″); 21.4 (C-1″) 17.9 (C-2′), 11.1 (C-3′).

Preparation of 5,6-dimethoxy-1-propyl-2,3,7,8,9,9a-hexahydro-1H-benzo[de]quinolin-7-one (47). Dry, finely powdered **46** (0.96 g, 2.79 mmol) was sprinkled over the surface of stirred oleum (6 mL; 20% free sulfur trioxide) at room temperature. The reaction mixture was stirred for a further 5 min. It was then quenched with ice and the solution basified to pH 11 with 32% sodium hydroxide solution. The basic solution was extracted with dichloromethane (3×50 mL), the extracts combined, dried and the solvent evaporated to leave 5,6-dimethoxy-1-propyl-2,3,7,8,9,9a-hexahydro-1*H*-benzo[*de*]-quinolin-7-one (**47**) as a dark green gum (0.61 g, 2.12 mmol, 74%). MS (CI): *m/z* 290 (MH$^+$, 100). HRMS (EI): *m/z* 288 (M-H$^+$, 16%, accurate mass 288.1599. $C_{17}H_{22}NO_3$ requires 288.160). ^{1}H NMR δ: 6.842 (s, 1H, ArH); 3.864, 3.852 (s, 6H, 2×Ar-OCH_3); 3.33 ('apparent doublet', J = 11.6 Hz, 1H, H-9a); 3.203–3.157 (m, 1H); 3.111–2.948 (m, 1H); 2.832–2.379 (m, 7H); 1.712–1.562 (m, 3H); 0.936 (t, J = 6.8 Hz, CH_3). ^{13}C NMR δ: 196.9 (C-7); 151.8 (C-6); 147.5 (C-5); 133.4 (C-6a); 129.4 (C-9b); 125.6 (C-3b); 116.7 (C-4); 61.3 (C-9a); 59.7, 55.9 (2×Ar-OCH_3); 55.1 (C-2); 49.1 (C-1′); 36.4 (C-8); 28.7, 27.3 (C-3, C-9); 19.4 (C-2′); 11.8 (C-3′).

Synthesis of 1,2-dimethoxy-6-propyl-5,6,6a,7-tetrahydro-4*H*-benzo[*de*][1,2,3]thiadiazolo[4,5-*g*]quinoline (39). Anhydrous sodium ethanoate (180 mg, 3.0 mmol) was added to a hot solution of semicarbazide hydrochloride (180 mg, 1.6 mmol) in ethanol (20 mL). The sodium chloride precipitate which formed was removed by filtration. To the filtrate was added the amino ketone **47** (360 mg, 1.2 mmol) and this mixture was heated under reflux for 1 h. After cooling, the solid was filtered, washed with cold ethanol and dried to afford, after recrystallisation from methanol, the semicarbazone **48** (180 mg, 0.5 mmol, 42%) m.p. 188.7–189 °C. MS (CI): *m/z* 347 (MH$^+$, 100%). HRMS (ES): *m/z* 347 (MH$^+$, 100%, accurate mass 347.2081. $C_{18}H_{27}N_4O_3$ requires 347.2083). ^{1}H NMR δ: 9.392 (s, 1H, NH), 6.624 (s, 1H, H-4), 3.849, 3.773 (s, 6H, 2×ArO-CH_3), 3.237–2.985 (m, 3H), 2.910–2.335 (m, 7H), 2.041 (s, 2H, NH_2), 1.750–1.280 (m, 3H), 0.995–0.890 (t, 3H, CH_3). ^{13}C NMR δ: 159.0 (C=O), 151.9 (C-5), 145.4 (C-6), 143.9 (C-7), 130.3 (C-3a), 128.46 (C-6b), 124.9 (C-6a), 112.5 (C-4), 60.7, 59,6 (2×Ar-OCH_3), 55.8 (C-9a), 55.5 (C-8), 48.7 (C-2), 28.5 (C-3), 26.0 (C-1′), 25.0 (C-9), 19.2 (C-2′), 11.9 (C-3′).

To thionyl chloride (2 mL) was added the semicarbazone **48** (40 mg, 0.12 mmol) portionwise at 0 °C with stirring. The mixture was stirred for a further 3 h at 0 °C and then kept overnight at room temperature. Dichloromethane (25 mL) was added and the mixture was poured with stirring into a cooled solution of sodium carbonate (6 g in 25 mL of water). The organic phase was separated, dried and the dichloromethane evaporated to give crude product. The crude product was purified via flash column chromatography (silica

gel, methanol:dichloromethane 5:95). Recrystallisation from methanol gave 1,2-dimethoxy-6-propyl-5,6,6a,7-tetrahydro-4*H*-benzo[*de*][1,2,3]thiadiazolo[4,5-*g*]quinoline (**39**) (8 mg, 0.02 mmol, 16%); m.p. 185–186 °C. MS (CI): *m*/*z* 332 (MH^+, 100%). HRMS (ES): *m*/*z* 332 (MH^+, 79%, accurate mass 332.1432. $C_{17}H_{22}N_3O_2S$ requires 332.1433). ^{1}H NMR δ: 6.711 (s, 1H, H-4); 3.987, 3.900 (s, 6H, Ar-OCH_3); 3.727 (dd, $J_1 = 6.0$, $J_2 = 15.0$ Hz, 1H, H-6a); 3.56–3.50 (dd, $J_1 = 3.0$, $J_2 = 15.0$ Hz, 1H, one of C-7); 3.24–3.16 (m, 1H, one of C-5); 3.122–3.014 (m, 1H, one of C-5); 2.90–2.647 (m, 2H, CH_2); 2.587–2.430 (m, 2H, CH_2); 1.639–1.543 (m, 2H, C-2′); 0.955 (t, $J_1 = 6.0$ Hz, 3H, C-3′). ^{13}C NMR δ: 152.6 (C-10a), 147.7 (C-7a, Ar-OCH_3), 144.2 (Ar-OCH_3), 130.8 (C-10b), 125.2 (C-10c), 121.6 (C-3a), 112.8 (C-3), 61.5 (C-6a), 59.2 (C-7), 56.3, 56.0 (2×Ar-OCH_3), 49.4, 29.1 (C-1′, C-3), 26.3 (C-4), 19.4 (C-2′), 12.0 (C-3′).

Preparation of 1,2,9-trimethoxy-6-propyl-4,5,6,6a,7,12-hexahydroisoquinolino[8,1-ab]carbazole (40). To a solution of the ketone **47** (1.2 g, 4.2 mmol) in dry ethanol (2.5 mL) and glacial acetic acid (three drops) was added fresh *p*-methoxyphenylhydrazine (0.36 g, 7.5 mmol) in dry methanol (2 mL). The reaction mixture was refluxed for 2 h under nitrogen and then the solvents evaporated. To the residue was added glacial acetic acid (4 mL) and redistilled boron trifluoride etherate (0.5 mL). The mixture under nitrogen was brought to reflux as rapidly as possible and heated for 10 min. Ice was added (50 g), the solution was basified to pH 11 with 32% sodium hydroxide solution, and the mixture was then extracted with chloroform (3×20 mL). The extracts were combined, washed with water and dried. Evaporation of the solvent afforded the crude product as a cream foam (1.05 g, 2.6 mmol, 64%). Recrystallisation from dichloromethane/light petroleum afforded 1,2,9-trimethoxy-6-propyl-4,5,6,6a,7,12-hexahydroisoquinolino[8,1-*ab*]carbazole **40** as tan crystals; m.p. 120–122 °C (Found; C, 73.2; H, 7.2; N, 7.2. $C_{24}H_{28}N_2O_3$ requires C, 73.4; H7.2; N, 7.1%). MS (CI): *m*/*z* 393 (MH^+, 100%). HRMS (EI): *m*/*z* 392 (M^+, 100%, accurate mass 392.212. $C_{24}H_{28}N_2O_3$ requires 392.210) 391 (71), 390 (52), 377 (61), 375 (27), 346 (21), 303 (23). ^{1}H NMR δ: 9.243, (s, 1H, NH); 7.311, (d, $J = 8.8$ Hz, 1H, ArH); 7.032, (s, 1H, ArH); 6.858 (d, $J = 8.7$ Hz, 1H, ArH); 6.519, (s, 1H, H-3); 3.901, (s, 3H, Ar-OCH_3); 3.877 (s, 6H, 2×Ar-OCH_3); 3.682–3.624, (m, 1H); 3.408–3.337, (m, 1H); 3.232–2.942, (m, 3H); 2.671–2.514, (m, 4H); 1.663–1.593, (m, CH_2); 0.997, (t, $J = 7.2$ Hz, CH_3). ^{13}C NMR δ: 154.2 (C-1), 151.0 (C-2), 142.3 (C-9), 131.5, 131.2 (C11a, C12a), 126.5 (C-7b), 126.2 (C-12c), 121.4 (C-12b), 112.6 (ArH), 112.0 (ArH), 110.6 (ArH), 99.9 (ArH), 60.8 (C-6a), 60.1 (Ar-OCH_3), 56.0 (CH_2), 55.9, 55.7 (2×Ar-OCH_3), 47.3 (C-1′), 41.5 (C-5), 29.4 (C-7), 25.2 (C-4), 18.9 (C-2′), 12.1 (C-3′).

Pharmacological tests. This testing was undertaken at the Victor Chang Cardiac Research Institute, Sydney, Australia. COS-1 membranes were prepared as described in the literature.[41] The cDNAs encoding the human α_1-adrenergic receptors were sub-cloned into the mammalian expression vector pMT2′.[41] Plasmid DNA was used to transfect cells. Transient expression in COS-1 cells was accomplished by the diethylaminoethane-dextran method.[42] The ligand binding characteristics of the expressed receptors were determined in a series of radioligand binding studies using the α_1-antagonist radioligand [^{125}I]HEAT as described previously.[41] Nonspecific binding was determined in the presence of 10^{-4} M phentolamine. Binding data were analysed by the iterative curve-fitting program LIGAND.

Molecular electrostatic potential mapping. This particular molecular modeling work was performed on a Silicon Graphics Indy workstation using Spartan SGI version 4.0.3. GL software, under the IRIX 5.2 system. The ligands were built and optimised by using an ab initio calculation at the Hartree–Fock level with the minimal STO-3G basis set. The electron density of the molecules was also calculated in three dimensions generating the isosurface (0.002 electron/au^3) and the electrostatic potential at each point was then determined and visualised colour coded onto this surface from the most negative (red) to the most positive (blue) values.

Catalyst experiments

All molecular modelling work was performed on a Silicon Graphics O_2 workstation using the Catalyst package of Molecular Simulations, Inc. (version 4.0), under an IRIX 6.3 operating system. A generalised CHARMM-like[36] force field was used throughout.

Training sets were selected as described in the Results section. Molecules were built within Catalyst and conformational models for each compound were generated automatically using the poling algorithm.[37,38] This emphasises representative coverage over a 20 kcal/mol energy range above the estimated global minimum and the 'best searching procedure' was chosen. The training subset of molecules with their associated conformational models and activities was submitted to Catalyst by using the 'generate hypothesis' command. The chemical functional groups used in this generation step included hydrogen bond donor and acceptor, hydrophobic, positive ion and aromatic ring groups. The statistical relevance of the various hypotheses so obtained was assessed on the basis of their cost relative to the null hypothesis and their correlation coefficients *R*.[37,38] The null hypothesis is an ideal hypothesis which is the simplest possible hypothesis that fits the data and for which there is no statistically significant structure including that the experimental activities are normally distributed about their mean. The cost function consists of two terms. The first penalises the deviation between the estimated activity and the experimental activity and the second penalises the complexity of the hypothesis. The hypotheses were then used to estimate the activities of the test compounds. These activities are derived from those conformers displaying the smallest root-mean square (RMS) deviations when projected onto the hypothesis.

Acknowledgements

The award of a scholarship from Zonguldak Karaelmas University in Turkey to Burak Coban, and research

support from the ARC and NHMRC are gratefully acknowledged. We also thank Professor R. M. Graham and colleagues at the Victor Chang Cardiac Research Institute, Sydney, Australia for the receptor binding assays. The input of the late Dr. E. J. Browne (University of Tasmania) into this project was also invaluable.

References and Notes

1. Beck-Sickinger, A. *Drug Discovery Today* **1996**, *1*, 502.
2. Graham, R. M.; Perez, D. M.; Piasciks, M. T.; Riek, R. P.; Hwa, J. *Pharmacol. Commun.* **1995**, *6*, 15.
3. Hieble, J. P.; Bondinell, W. E.; Ruffolo, Jr., R. R. *J. Med. Chem.* **1995**, *38*, 1838.
4. Ruffolo, Jr., R. R.; Bondinell, W.; Hieble, J. P. *J. Med. Chem.* **1995**, *38*, 3681.
5. Alexander, S. P. H.; Peters, J. A. Eds., The 1998-receptor and ion channel nomenclature supplement, In: *Trend. Pharmacol. Sci.* 9th, Elsevier Trends Journals: Cambridge, 1998.
6. Bylund, D. B.; Eikenberg, D. C.; Hieble, J. P.; Langer, S. Z.; Lefkowitz, R. J.; Minneman, K. P.; Molinoff, P. B.; Ruffolo, Jr., R. R. *Trendelenburg, U. Pharmacol. Rev.* **1994**, *46*, 121.
7. Forray, C.; Wetzel, J. M.; Branchek, T. A.; Bard, J. A.; Chiu, G.; Shapiro, E.; Tang, R.; Lepor, H.; Hartig, P. R.; Weinshank, R. L.; Gluchowski, C. *Mol. Pharmacol.* **1994**, *45*, 703.
8. Gluchowski, C.; Wetzel, J. M.; Chiu, G.; Marzabadi, M. R.; Wong, W. C.; Nagarathnam, D. International Patent No. WO 94/22829, 1994.
9. Konkel, M. J.; Wetzel, J. M.; Cahir, M.; Craig, D.; Noble, S. A.; Gluchowski, C. The 216th ACS National Meeting, Boston, 23–27 August, 1998, MEDI#129.
10. Meyer, M. D.; Altenbach, R. J.; Basha, F. Z.; Carroll, W. A.; Drizin, I.; Elmore, S. W.; Ehrlich, P. P.; Lebold, S. A.; Tietje, K.; Sippy, K. B.; Wendt, M. D.; Plata, D. J.; Plagge, F.; Buckner, S. A.; Brune, M. E.; Hancock, A. A.; Kerwin, J. F., Jr. *J. Med. Chem.* **1997**, *40*, 3141.
11. Giardina, D.; Crucianelli, M.; Melchiorre, C.; Taddei, C.; Testa, R. *Eur. J. Pharmacol.* **1995**, *287*, 13.
12. Testa, R.; Guarnery, L.; Angelico, P.; Poggesi, E.; Taddei, C.; Sironi, G.; Colombo, D.; Sulpizio, A. C.; Naselsky, D. P.; Hieble, J. B.; Leonardi, A. *J. Pharmacol. Exp. Ther.* **1997**, *281*, 1284.
13. Kenny, B.; Ballard, S.; Blagg, J.; Fox, D. *J. Med. Chem.* **1997**, *40*, 1293.
14. Gluckowski C. The discovery of selective α_{1A} antagonists using recombinant human α_1-adrenoceptors. IBC-GPCR Conference, Philadelphia, PA, 11–13 December 1995.
15. Foglar, R.; Shibata, K.; Horie, K.; Hirasawa, A.; Tsujimuto, G. *Eur. J. Pharmacol.* **1995**, *288*, 201.
16. King, H. K.; Goetz, A. S.; Ward, S. D. C.; Saussy, Jr., D. L. *Soc. Neuro. Abs.* **1994**, *20*, 526.
17. DeBenedetti, P. G.; Fanelli, F.; Menziani, M. C.; Cocchi, M.; Testa, R.; Leonardi, A. *Bioorg. Med. Chem.* **1997**, *5*, 809.
18. Ko, F. N.; Guh, J. H.; Yu, S. M.; Hou, Y. S.; Wu, Y. C.; Teng, C. M. *Br. J. Pharmacol.* **1994**, *112*, 1174.
19. Ford, A. P. D. W.; Williams, T. J.; Blue, D. R.; Clarke, D. E. *Trend. Pharmacol. Sci.* **1994**, *15*, 167.
20. Phife, D. W.; Ramos, R. A.; Feng, M.; King, I.; Gunasekera, S. P.; Wright, A.; Patel, M.; Pachter, J. A.; Coval, S. J. *Bioorg. Med. Chem. Lett.* **1996**, *6*, 2103.
21. De Marinis, R. M.; Wise, M.; Hieble, J. P; Ruffolo, Jr., R. R. In *The alpha-1 Adrenergic Receptor*; Ruffolo, Jr., R. R. Ed.; Humana Press: New Jersey, 1987; pp. 211–258.
22. DeBenedetti, P. G.; Fanelli, F.; Menziani, M. C.; Cocchi, M. *J. Mol. Struc.* **1995**, *305*, 101.
23. Cocchi, M.; Fanelli, F.; Menziani, M. C.; DeBenedetti, P. G. *J. Mol. Struc.* **1995**, *331*, 79.
24. Venturelli, M.; Menziani, M. C.; Cocchi, M.; Fanelli, F.; DeBenedetti, P. G. *(Theochem)-Journal of Molecular Structure* **1992**, *276*, 327.
25. Bremner, J. B.; Coban, B.; Griffith, R. *J. Comp. Aid. Mol. Des.* **1996**, *10*, 545.
26. Shamma, M. *The Isoquinoline Alkaloids*. Chemistry and Pharmacology Academic Press Inc: New York, 1972.
27. Madrero, Y.; Elorriaga, M.; Martinez, S.; Noguera, M. A.; Cassels, B. K.; D'Ocon, P.; Ivorra, M. D. *Brit. J. Pharmacol.* **1996**, *119*, 1563.
28. Groenewoud, K. M. Ring-D aporphine analogues. B.Sc. honours thesis, Department of Chemistry, University of Tasmania, 1991.
29. Sleight, A. J.; Koek, W.; Bigg, D. C. H. *Eur. J. Pharmacol.* **1993**, *238*, 407.
30. Wetzel, J. M.; Salon, S. A.; Tamm, J. A.; Forray, C.; Craig, D.; Nakanishi, H.; Cui, W.; Vaysse, P. J. J.; Chiu, G.; Weinshank, R. L.; Hartig, P. R.; Branchek, T. A.; Gluchowski, C. *Receptors and Channels* **1996**, *4*, 165.
31. Hamaguchi, N.; True, T. A.; Saussy, D. L.; Jeffs, P. W. *Biochemistry* **1996**, *35*, 14313.
32. Brossi, A.; Dolan, L. A.; Teitel, S. *Org. Synth.* **1977**, *56*, 3.
33. Berney, D. *Helv. Chim. Acta* **1982**, *65*, 1694.
34. Bremner, J. B.; Browne, E. J. *J. Heterocyc. Chem.* **1975**, *12*, 301.
35. Greene, J.; Kahn, S.; Savoj, H.; Sprague, P.; Teig, S. *J. Chem. Inf. Comp. Sci.* **1994**, *34*, 1297.
36. Brooks, B. R.; Brucolleri, R. E.; Olafson, B. D.; States, D. J.; Swaminathan, S.; Karplus, M. *J. Comput. Chem.* **1983**, *4*, 187.
37. Smellie, A.; Kahn, S. D.; Teig, S. L. *J. Chem. Inf. Comp. Sci.* **1995**, *35*, 285.
38. Smellie, A.; Kahn, S. D.; Teig, S. L. *J. Chem. Inf. Comp. Sci.* **1995**, *35*, 295.
39. Griffith, R.; Bremner, J. B.; Coban, B. In *Pharmacophore Perception, Development, and Use in Drug Design*; Guner, O., Ed.; International University Line: La Jolla, in press.
40. Perrin, D. D.; Armarego, W. L. F. *Purification of Laboratory Chemicals*. 3rd Ed. Pergamon Press: Oxford.
41. Perez, D. M.; Piascik, M. T.; Graham, R. M. *Mol. Pharmacol.* **1991**, *40*, 876.
42. Sambrook, J.; Fritsch, E. F.; Maniatis, T. *Molecular cloning: A laboratory manual*. Cold Spring Harbor Laboratory: Cold Spring Harbour, New York, 1989.